ULTRAVIOLET RAMAN SPECTRAL SIGNATURES IN SUPPORT OF LISA (LASER INTERROGATION OF SURFACE AGENTS)

Arthur J. Sedlacek, III and Charles C. Finfrock
Brookhaven National Laboratory
Upton, NY

Steve Christesen
Edgewood Chemical Biological Center
Edgewood, MD

Tom Chyba and Scott Higdon
ITT Industries
Albuquerque, NM

ABSTRACT

SBCCOM/PNBC and ITT Industries are in a Cost-sharing venture on the development of LISA-Recon (Laser Interrogation of Surface Agents). This engineering, testing and evaluation effort uses a novel mini-Raman lidar technique for on-the-move, short-range, non-contact detection and identification of chemical agents on the battlefield. Unlike traditional lidar, LISA-Recon is specifically designed to analyze ground/surface contamination at a distance of approximately 1 meter. It is envisioned that the finished unit will reside on the NBCRS "Fox" vehicle. In support of this ongoing engineering effort, Brookhaven, Edgewood and ITT Industries have teamed up to procure the relevant Raman spectral signatures for various agents and their respective surrogates. A brief introduction to UV Raman spectroscopy along with selected spectral signatures, cross-sections and implications to the LISA technology will be presented.

INTRODUCTION

Both the purposeful deposition and persistence of chemical agents deposited on the battlefield and other surfaces presents a very significant threat to our military forces. In an effort to address this threat, BNL, ECBC, and ITT are collaborating on the transitioning of the BNL-developed Mini-Raman lidar System (MRLS),[1,2,3] to an instrument known as LISA (Laser Interrogation of Surface Agents). While the DOE-sponsored MRLS was developed for the First Responder community in an effort to provide these Haz/Mat professionals an in-field tool to assist in detecting and identifying unknown chemical spills[4], LISA is being specifically designed to interrogate the battlefield for chemical agent contamination. These unique instruments combined the active electro-optic technique known as light detection and ranging (lidar) with Raman spectroscopy to detect and identify chemicals on surfaces. Lidar is similar to radar. Pulses of laser light are sent to a target of interest and the backscattered signals are collected by a receiver telescope. Raman spectroscopy is a process where laser light scattered from a molecule carries

Report Documentation Page

Form Approved
OMB No. 0704-0188

1. REPORT DATE	2. REPORT TYPE	3. DATES COVERED
01 JUL 2003	**N/A**	**-**

4. TITLE AND SUBTITLE	5a. CONTRACT NUMBER
Ultraviolet Raman Spectral Signatures In Support Of Lisa (Laser Interrogation Of Surface Agents)	5b. GRANT NUMBER
	5c. PROGRAM ELEMENT NUMBER
6. AUTHOR(S)	5d. PROJECT NUMBER
	5e. TASK NUMBER
	5f. WORK UNIT NUMBER
7. PERFORMING ORGANIZATION NAME(S) AND ADDRESS(ES) **Brookhaven National Laboratory Upton, NY**	8. PERFORMING ORGANIZATION REPORT NUMBER
9. SPONSORING/MONITORING AGENCY NAME(S) AND ADDRESS(ES)	10. SPONSOR/MONITOR'S ACRONYM(S)
	11. SPONSOR/MONITOR'S REPORT NUMBER(S)

12. DISTRIBUTION/AVAILABILITY STATEMENT
Approved for public release, distribution unlimited

13. SUPPLEMENTARY NOTES
See also ADM001523., The original document contains color images.

14. ABSTRACT

15. SUBJECT TERMS

16. SECURITY CLASSIFICATION OF:			17. LIMITATION OF ABSTRACT	18. NUMBER OF PAGES	19a. NAME OF RESPONSIBLE PERSON
a. REPORT	b. ABSTRACT	c. THIS PAGE			
unclassified	**unclassified**	**unclassified**	**UU**	**9**	

Standard Form 298 (Rev. 8-98)
Prescribed by ANSI Std Z39-18

information about the chemical makeup of the molecule. The generated Raman signal is unique to each molecule. Just as people can be uniquely identified through their respective fingerprints, so too can chemicals with Raman spectroscopy, regardless of their physical state (solid, liquid, gas). The result is a unique chemical fingerprint.

The present paper is focused on the acquisition of much needed deep UV spectral fingerprints in support of the LISA R&D effort.[5] This spectral databasing effort is necessary for two reasons. First, there is a complete lack of deep UV Raman spectral fingerprints for the chemicals of interest for spectral pattern matching purposes (i.e., chemical identification). Second, deep UV excitation can result in the observation of pre-resonance and resonance-enhanced Raman scattering that can result in (i) the alteration of relative Raman mode intensities as well as (ii) the appearance of new Raman peaks. It is because of this latter reason that the extrapolation of NIR-Raman spectra cannot be used by simply applying the ν^4-frequency dependence law, but that rather actual, well-controlled measurements must be carried out.

BACKGROUND

In contrast to Rayleigh scattering, Raman scattering is an inelastic process (i.e., energy is either lost or gained upon a photon/molecule collision). Raman scattering is a two photon process that has gone in and out of favor since its first observation by C. V. Raman some 65 years ago.[6] In this inelastic process, an exciting photon of energy $h\nu$ is absorbed, promoting a molecule to a virtual level. With the sole requirement that this level be energetically distant from the real level (i.e., large δE) the uncertainty principle allows the lifetime of this state to be vanishingly small resulting in the instantaneous emission of a second photon to either its original state (Rayleigh scattering) or, is shifted in frequency, to a different real state (Raman scattering). If the final state lies above the initial state than the observed lines are referred to as Stokes, and anti-Stokes if they lie below. In this way Raman spectra will reflect the molecular vibrational transitions that provide the same kind of molecule identification information as infrared (IR) spectra. Since water is a poor Raman scatterer, it is a simple matter to procure a Raman fingerprint in a variety of environmental conditions. In addition, the Raman fingerprint is independent of the excitation frequency allowing its use in the solar-blind spectral region and its lines are typically fewer in number and sharper than IR lines, thereby providing better identification capability of compounds in mixtures and solutions. Finally, the ν^4-dependence of the scattering cross-section on excitation frequency observed in normal Raman spectroscopy can undergo further enhancement when the excitation frequency approaches an electronically excited state of the molecule.[7] This enhancement, which can range from 1 to 4 orders of magnitude, is referred to as resonance Raman (RR), since the excitation frequency is in "resonance" with an allowed electronic transition. This improvement in the cross-section, in conjunction with the global advantages of Raman spectroscopy cited earlier, provide an optical open-path platform for the remote sensing of toxic chemicals and hazardous wastes. Finally, this scattering technique has equal applicability with gases, liquids or solids.

EXPERIMENTAL METHODS

Figure 1 is a schematic diagram of the experimental apparatus used to measure Raman cross sections. A Spectra- Physics MOPO-730 system generates continuously tunable radiation from 410 nm to 2000 nm. The MOPO-730 is a BBO-based optical parametric oscillator (OPO) pumped by the third harmonic ~355 nm of a 30 Hz Nd:YAG laser. The UV light (210–400 nm) is obtained by doubling either the signal or the idler beam from the MOPO. The pulse width of the UV light is 3–4 ns, and the linewidth is approximately 0.3 cm^{-1}.

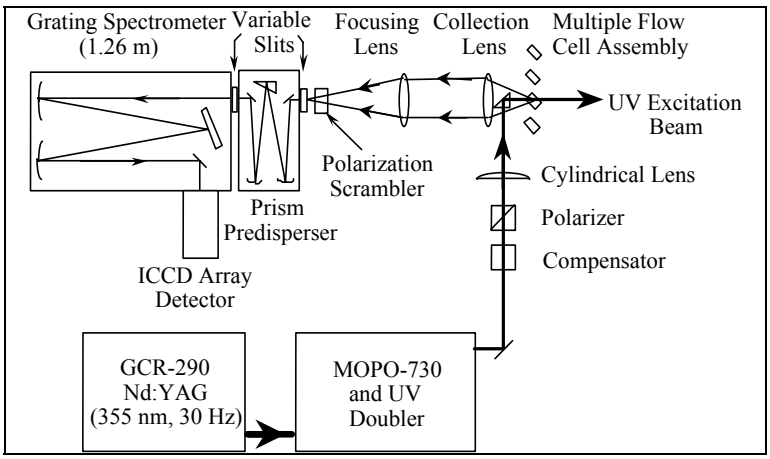

Figure 1. Schematic of Experimental Setup Used to Collect UV Raman Signatures

A 254 mm focal length cylindrical lens focuses the excitation light into the sample. The UV energy is 0.5 mJ/pulse or less, and the spot size at the sample is approximately 0.733 mm. The scattered light is collected at 180° with respect to the incident UV beam by a 50.8 mm diameter spherical lens (*f* number=1). The angle between the UV beam and the surface of the sample stream is 45° to reduce back reflections from the cell walls. Another 50.8 mm dia spherical lens focuses the scattered light into the prism predisperser. The *f* number of the second lens matches the *f* number of the prism predisperser and spectrometer for maximum throughput of the scattered light. The predisperser works as a sharp-cut bandpass filter with high throughput (40%–50%) and negligible aberration.

The spectrometer is a 1.26 m single stage monochromator (Spex Model 1269) with a 1800 grooves/mm grating. The width of the entrance slit in the spectrometer is controlled to reject elastically scattered laser light, while the resolution of Raman spectra is governed by the slit width of the predisperser. With this combination, we are able to measure Raman shifts of less than 200 cm^2 in deep UV with negligible Rayleigh background. A crystalline quartz wedge polarization scrambler in front of the entrance slit of the predisperser depolarizes the polarized Raman signal before it enters the spectrometer.

The optical throughput of both the predisperser and the spectrometer have been measured at various wavelengths in the UV using a NIST standard D_2 lamp. The spectra of the standard Hg lamp and known chemicals serve as wavelength calibrations for the predisperser and the monochromator.

The Raman spectra are captured by a gated, intensified CCD detector (Oriel Instaspec V, 1024X256 pixel array, 25 mm (and 18 mm) window width) mounted at the exit port of the spectrometer. The CCD chip is cooled to -25 °C (-35 °C) to yield a dark count of less than $2x10^{-5}$ counts $element^{-1}$ s^{-1}. The adjustable gain of the intensifier is set to ~50 counts/photoelectron (150 counts/photoelectron) for all measurements. The Raman spectra are normalized to the measured response uniformity of the ICCD array.

SAMPLE HANDLING FOR UV RAMAN SPECTROSCOPY

Preparation and handling of samples for analysis by UV Raman spectroscopy was conducted using the procedures, protocols and methods described below. Chemicals used in the analysis were obtained from reputable commercial research chemical suppliers. They were obtained in the highest purity commonly available to the research community. Certificates of analysis were obtained from the vendor for virtually all of the chemicals used in this project. Chemical purity was verified in-house by gas

chromatography (HP 5890 Series 2 chromatograph outfitted with a 25 m x 0.32 x 0.52 μm FFAP capillary column) for all tested liquids except SF-96 and HPLC grade water. In order to preserve the purity of the chemicals tested, only certain container and sample handling materials were permitted. Acceptable sample handling materials were glass, Teflon, PFA (perfluoro (alkoxyalkane) copolymer), PEEK (polyaryl ether ether ketone) and stainless steel, all of which were subjected to the following cleaning protocol. All materials were ultrasonically cleaned in warm distilled water and ultrasonic cleaner detergent solution for a minimum of fifteen minutes. The materials were then rinsed with copious amounts of distilled water and then rinsed with spectroscopic grade methanol, followed by drying in an 80^{o}C glassware-drying oven. The only departure from this protocol was the method for cleaning the magnetic drive pumps used with the windowless flow cell. As these pumps have interior spaces that are not easily accessible for cleaning, sufficient pumps were obtained to allow compatible chemicals to have dedicated pumps. In the event that a pump did require cleaning, the following method was applied. The pump was allowed to pump itself dry into a waste vessel. Several aliquots of appropriate solvents were cycled through the pumps alternated with drying of the interior with dry filtered compressed air. This was done over the course of several hours. The final rinse of a pump was with a solvent of high vapor pressure, such as cyclohexane, which was then easily removed by flowing dry filtered compressed air through the pump for several hours while it was slowly rotating.

Some samples required dilution prior to analysis. Dilutions, when required, were prepared gravimetrically using a Mettler AE 100 or a Mettler SB 8001 electronic balance, as dictated by the amount of sample being prepared. Concentrations are expressed in terms of weight percent, in other words, mass of minor component divided by total mass, times 100.

In order to address potential reabsorption, UV/VIS absorption spectra of all samples were collected with a Perkin-Elmer 320 spectrophotometer. In addition to this, NIR Raman spectra were collected using a Bruker IFS-66 FT spectrometer outfitted with a NIR Raman attachment (FRA-106).

Two sample-handling systems were developed to facilitate liquid sample exposure to the UV Raman spectroscopy system. A closed system using quartz flow cells and a syringe pump was developed, as well as a "windowless" system consisting of an open flow cell and small magnetic drive chemical pumps. The closed system consisted of a Harvard Apparatus "33" syringe pump, an array of ten milliliter glass syringes, a set of four-way control valves, a collection of quartz flow cells of varying path length, a set of glass sample reservoirs, required connecting tubing, and a positioning system to locate the cells in the beam path. The syringe pump was programmed to alternately draw and push the sample between the reservoir and syringe body via the connecting tubing and the quartz cell. This system provided a completely closed environment for the sample with good control of the flow rate and path length. Evaporation of samples with high vapor pressure was well suppressed in this system. A disadvantage of this system was the spectroscopic contribution of the quartz cells containing the samples. The "windowless" sample introduction system circumvented this problem. The "windowless" system consisted of an array of magnetic drive chemical pumps from Micropump® Corp., an array of glass sample reservoirs, appropriate connecting tubing, and a specially fabricated Teflon and glass cell. The upper member of the cell is machined from Teflon and is a hollow cylinder with a narrow slot milled along the diameter of the end. At each end of the slot, small glass rods are inserted into drilled holes that terminate the ends of the slot. This is mounted in a fixture so that the slot and glass rods point vertically downward. Immediately below the glass rods is a Teflon well that has a PFA compression fitting below for attachment of a glass sample reservoir. The pump is connected to draw sample from the bottom of the reservoir and deliver it to the interior of the upper Teflon member. The sample flows out of the slot and wets the glass rods, forming a falling film or sheet of sample, which is collected back into the reservoir by the well. This assembly may be mounted to the same positioning system as the quartz cells described above, and is typically positioned so that the beam passes through the falling film formed between the glass rods. This system has the advantage of eliminating any contribution to the spectrum by cell

materials In the beam path, but the flow rate and sample film characteristics are somewhat dictated by the sample's surface tension and wetting characteristics.

Solid samples were fixed to the positioning system used for the cells above by appropriate clamps, and positioned in the beam manually.

RESULTS AND DISCUSSION

For Raman scattering in a molecule from an initial vibronic state $|m\rangle$ to a final state $|n\rangle$, the observed signal is

$$I_{mn} = N_m \cdot \sigma_{mn}(\nu_0) \cdot I_0 \cdot F(\theta) \cdot S(\nu_R) \cdot E(\nu_R) \cdot D(\nu_R), \quad (1)$$

where ν_0 and ν_R are the excitation and Raman frequencies, N_m is number of molecules in state $|m\rangle$ within the detection volume, I_0 is the laser intensity, $F(\theta)$ is the optical collection efficiency, $S(\nu_R)$ is the transmittance of the Raman signal from within the sample, $E(\nu_R)$ is the throughput of the spectrometer, and $D(\nu_R)$ is the detector response. The differential Raman cross-section $\sigma_{mn}(\nu_0)$ is,

$$\sigma_{mn}(\nu_0) = \frac{2^7 \cdot \pi^5}{3^2} \cdot \nu_0 (\nu_0 - \nu_{mn})^3 \cdot g \cdot f(T) \cdot \sum_{\rho\sigma} \left| (\alpha_{\rho\sigma})_{mn} \right|^2 \quad (2)$$

The term ν_{mn} is the frequency of the Raman vibrational mode, g is the degeneracy of the initial state $|m\rangle$, *f(T)* is the Boltzmann weighting factor specifying the thermal occupancy of the initial state, and $\alpha_{\sigma\rho}(\nu_0)$ is a component of the Raman polarizability tensor for the excitation frequency ν_0, averaged over all molecular orientations.

With respect to an external standard, the differential Raman cross-section of the sample is

$$\sigma_S(\nu_{mn}) = \sigma_R(\nu_{m'n'}) \cdot \left(\frac{I^S_{mn}}{I^R_{m'n'}} \right) \cdot \left(\frac{N_R \cdot I_0^R \cdot F(\theta)_R \cdot S(\nu_{m'n'})_R \cdot E(\nu_{m'n'})_R \cdot D(\nu_{m'n'})_R}{N_S \cdot I_0^S \cdot F(\theta)_S \cdot S(\nu_{mn})_S \cdot E(\nu_{mn})_S \cdot D(\nu_{mn})_S} \right) \quad (3)$$

where S and R denote the sample and reference. Since the pathlength of sample stream is much smaller than the focal length of the first collection lens, the refractive index dependent solid-angle correction has a negligible contribution (< 1%) to the cross-section. In addition, all Raman spectra collected must be corrected for the absorption of the excitation light and the Raman returns by the sample itself. The latter correction is referred to as self-absorption. For cross-section determination, both the internal and external methods are used. Standard chemicals whose cross-section as a function of excitation in the UV is known includes acetonitrile[8,9] cyclohexane[9] and water.[9] Finally, the purity levels of all procured chemicals (Aldrich, Sigma,) were certified and procured at the highest purity available. The purity was confirmed by in-house GC measurements (*vide supra*).

Shown in Figures 2-6 are example spectra collected for chemical and biological surrogates and one Schedule III agent. These spectra are selected to highlight specific aspects of deep UV Raman spectroscopy with an emphasis on pre-resonance and resonance-enhancement.

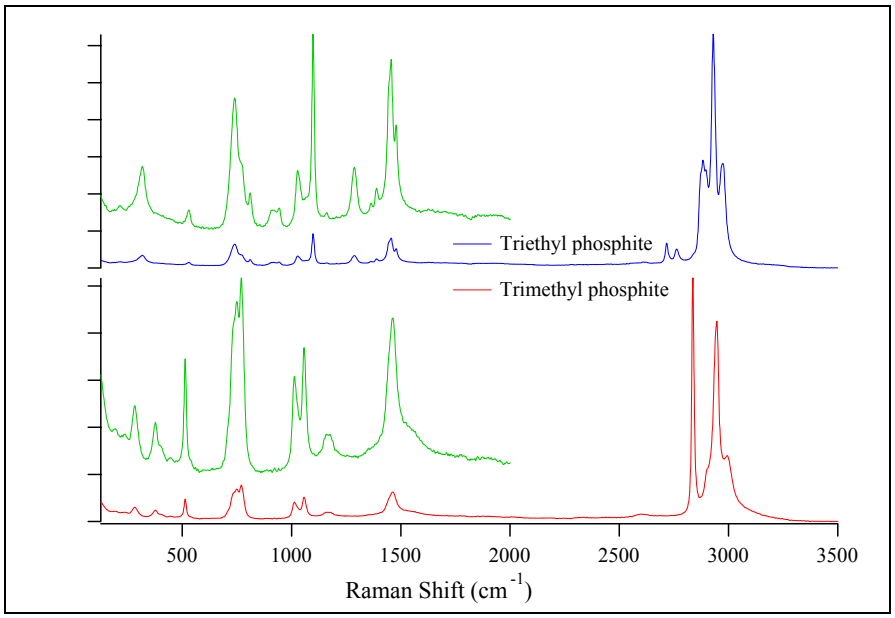

Figure 2. Raman spectra for trimethyl phosphite and triethyl phosphite, 2 schedule 3 agents. These structurally similar chemicals are readily distinguishable with Raman spectroscopy.

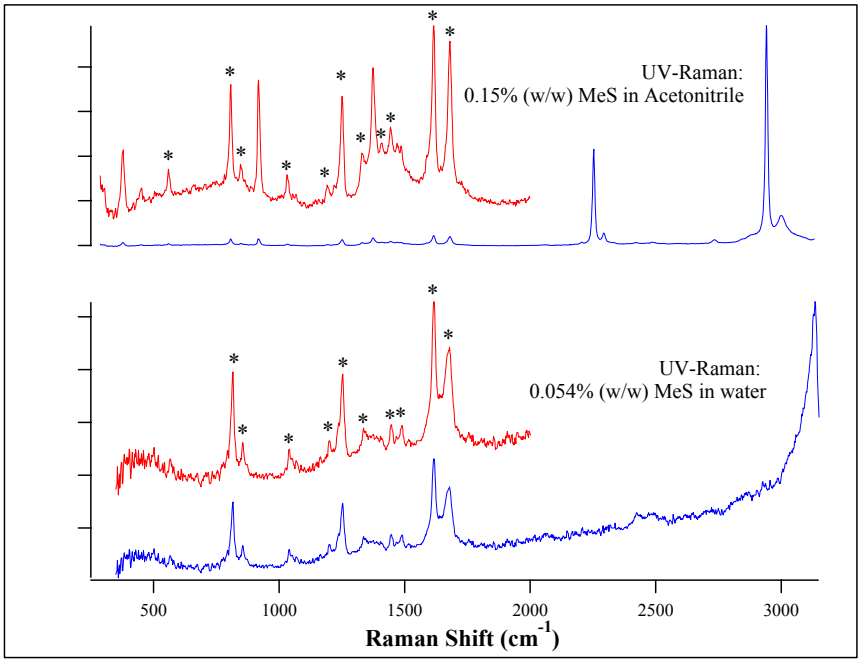

Figure 3. 248 nm excitation of methyl salicylate (MeS) in acetonitrile and water at 150 ppm and 54 ppm, respectively. These data demonstrate the sensitivity gain when UV-resonance enhancement is operational in a system.

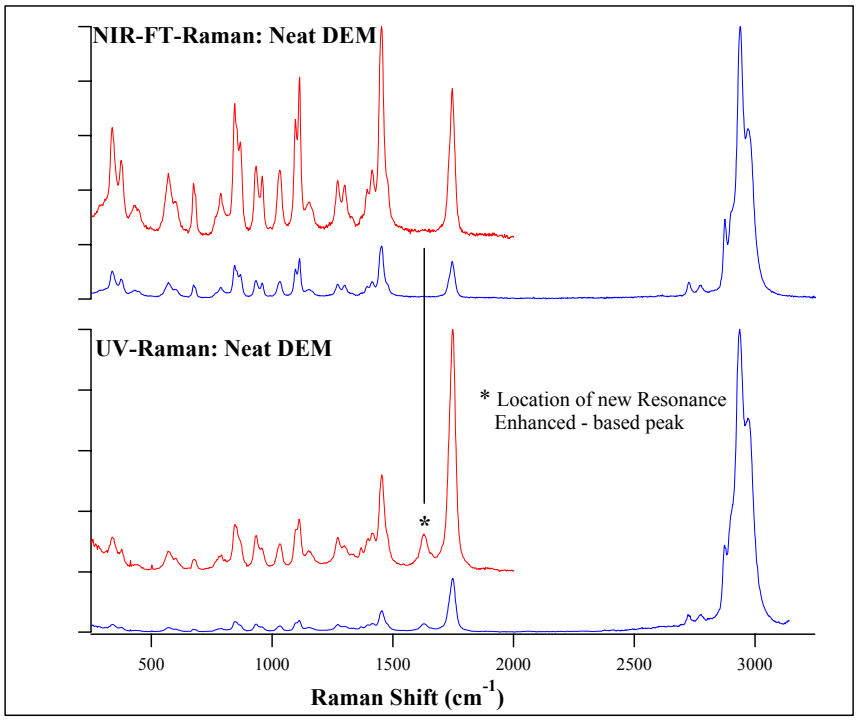

Figure 4. 248 nm excitation of diethyl malonate (DEM) in acetonitrile. These data demonstrate the appearance of new features when UV-resonance enhancement is operational in a system as well as changes in the relative peak intensities.

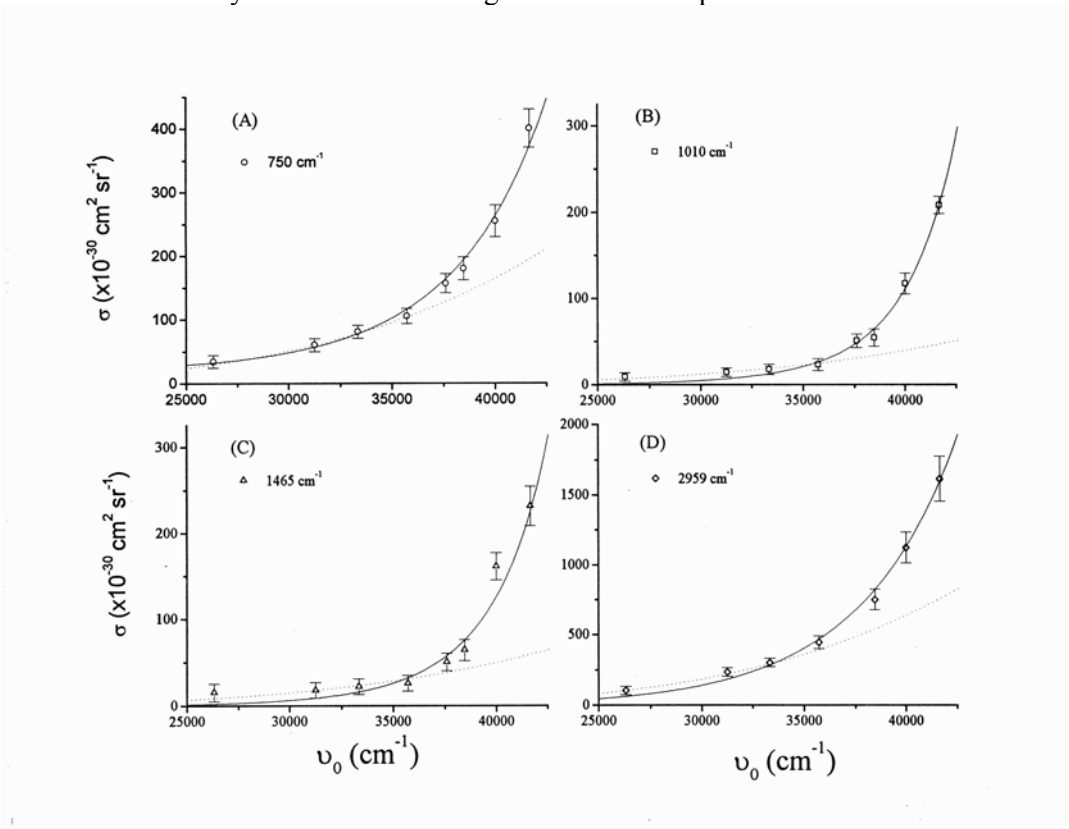

Figure 5. Scattering cross-section dependence for 4 modes of trimethyl phosphite as a function of UV excitation wavelength.

The excitation profiles of P-O stretch (750 cm^{-1}), O-C stretch (1010 cm^{-1}), CH_3 deformation (1464 cm^{-1}) and CH_3 stretch modes (2959 cm^{-1}) are shown. Experiments show only a slight *pre*-resonant effect for all the prominent TMP modes and that the pre-enhancement is different for the differing modes. These data imply that the different vibrational modes either couple differently to a given electronic state or that the different modes couple to different excited states.

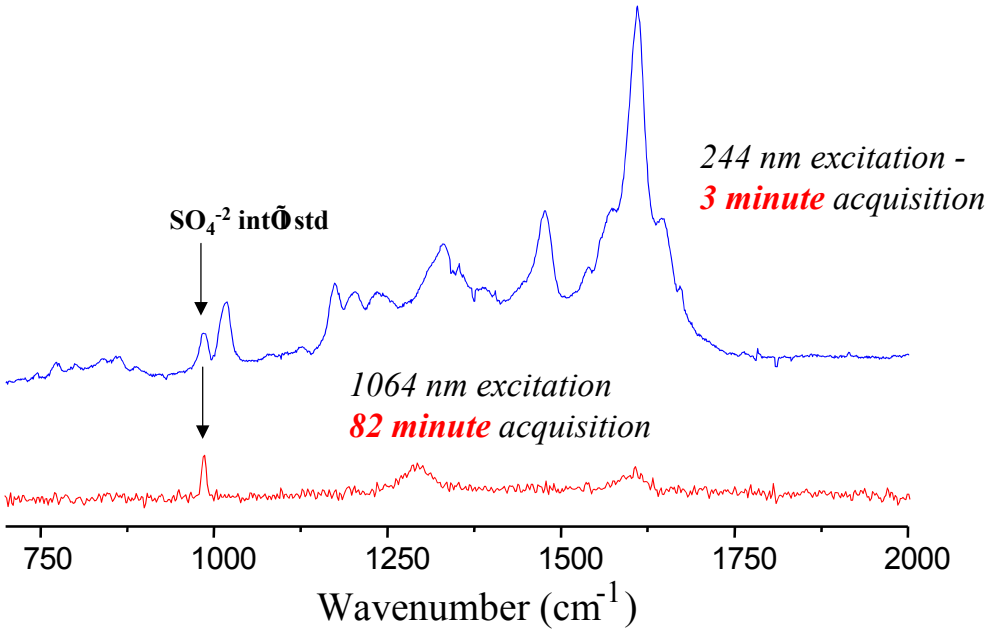

Figure 6. UVRR of *B*. Thuringiensis spores in 0.1 M Na_2SO_4 $2.6x10^8$ cfu/ml (~ 300 cells in detection volume). This spectrum demonstrates the increased sensitivity and information content available to resonance Raman spectra.

SUMMARY

BNL has been tasked with the measurement of deep UV Raman spectral fingerprints and associated scattering cross-sections of chemicals important in battlefield and associated surface contamination. This spectral databasing effort is in direct support of the SBCCOM/ITT cost-sharing R&D program to transition the mini-Raman lidar system to a LISA (Laser Interrogation of Surface Agents) platform for the battlefield detection of chemical agents on the ground with the NBCRS "Fox" vehicle. Examples of UVRR spectral for chemical and biological surrogates and one Schedule III agent were presented.

ACKNOWLEDGMENTS

Authors gratefully acknowledge the assistance of Dr. M. Wu on the acquisition of the TMP dataset.

REFERENCES

1. M. R. Ray, A. J. Sedlacek, M. Wu., Rev. Sci. Instru. **71** (9) 3485 (2000)

2. M. Wu, M. Ray, K. H. Fung, M. W. Ruckman, D. Harder, and A. J. Sedlacek III, J. Appl. Spectrosco. **54**, (6) 800 (2000)

3. A. J. Sedlacek, M. Ray and C. Ruth Kempf, Spectroscopic Detection and Identification Demonstration at New York City Chemical Agent Terrorist Exercise (ICE-FIELDEX) November 1997., DOE/NN-20 Report

4. A. J. Sedlacek, III and M. Wu. Trends in Appl. Spectro. (in press)

5. A. J. Sedlacek and C. C. Finfrock, UltraViolet Raman Spectral Signature Acquisition: UV Raman Spectral Fingerprints; ECBC Interim Report (Oct. 2002)

6. V. Raman and K. S. Krishnan, Nature **121**, 501 (1928)

7. See for example; D. A. Long, Raman Spectroscopy, McGraw-Hill: NY (1977)

8. M. Dudik, C. R. Johnson, and S. A. Asher, J. Chem. Phys. **82**, 1732 (1985)

9. Li and A. B. Myers, J. Phys. Chem. **94**, 4051 (1990)